Biomass Conversion and Biorefinery
https://doi.org/10.1007/s13399-023-04237-2

ORIGINAL ARTICLE

Two stages upgrading of bio-oil through esterification and hydrodeoxygenation reactions using Fe_2O_3-CoO supported catalyst

Ahmad Nasir Pulungan[1] · Ronn Goei[2] · Agus Kembaren[1] · Nurfajriani Nurfajriani[1] · Junifa Layla Sihombing[1] · Saharman Gea[3] · Hana Ria Wong[1] · Muhammad Irvan Hasibuan[1] · Rahayu Rahayu[1] · Alfred Iing Yoong Tok[2]

Received: 24 January 2023 / Revised: 5 April 2023 / Accepted: 17 April 2023

Abstract
Bio-oil contains many oxygenated compounds, as well as high acid and water content, which can reduce the stability of its components and have poor overall physicochemical properties. In this study, the quality of bio-oil produced from the pyrolysis of oil palm fronds was enhanced through a hydrodeoxygenation (HDO) reaction that was preceded by esterification as a pre-treatment. The catalyst used in the HDO reaction is mixed metal oxide (Fe_2O_3-CoO) anchored within zeolite mordenite (Fe_2O_3-CoO/Mor). The catalysts were characterized using XRD, SEM-EDX, and BET methods. The presence of metal oxides on the surface of mordenite increases the activity of the catalyst in producing liquid products while reducing the formation of coke. Upgrading of bio-oil has improved the physicochemical properties of bio-oil compared to the one-stage upgrading process. The analysis of product showed that the C and H content increased from 11.5 to 23.5 wt% and from 9.76 to 11.2 wt%, respectively. On the other hand, the O content decreased from 78.7 to 65.2 wt% with a degree of deoxygenation of 59.8%. Moreover, higher heating value (HHV) of the bio-oil increased by 38% from 11.6 to 16.0 MJ/kg.

Keywords Hydrodeoxygenation · Esterification · Palm frond bio-oil · Mordenite · Metal oxide

1 Introduction

Bio-oil is produced through the pyrolysis process of lignocellulosic biomass. Palm fronds, which contain acidic compounds (acetic acid), phenolic compounds (phenol, 2-methoxy phenol), aldehydes (2-furan-carboxaldehyde), and ketones (1-hydroxy-2-propanone), are one of the potential biomass resources [1]. However, bio-oil produced from pyrolysis cannot be directly used as fuel because its properties and characteristics have not yet met the required standards [2], as produced bio-oil is corrosive with high acidity and low heating value due to high water content [3, 4]. Moreover, it is unstable when stored at room temperature due to its high content of oxygenated compounds [5]. Bio-oil is prone to undergo changes as a result of oxidative and thermal degradation during storage [6]. Oxidation causes polymerization and thus increases the viscosity of bio-oil. On the other hand, thermal degradation causes partial decomposition of the components leading to the loss of volatile compounds in bio-oil.

Upgrading the quality bio-oil is important to make bio-oil more compatible for storage and subsequent processing into liquid fuel. Esterification of bio-oils produces bio-oils with greater stability and compatibility during storage, for example, via the formation of compounds like esters, accompanied with further purification processes [4, 7], whereas the conversion of bio-oil to fuel for transportation can be carried out via hydrodeoxygenation (HDO) method. HDO reaction required high operating temperature and pressure. HDO of biomass produces ketones and aldehydes, such as furfural,

✉ Ahmad Nasir Pulungan
nasirpl@unimed.ac.id

✉ Alfred Iing Yoong Tok
miytok@ntu.edu.sg

[1] Department of Chemistry, Faculty of Mathematics and Natural Sciences, Universitas Negeri Medan, Jl. Willem Iskandar Pasar V Medan Estate, Medan 20221, Indonesia

[2] School of Materials Science and Engineering, Nanyang Technological University, 50 Nanyang Avenue, Singapore 639798, Singapore

[3] Department of Chemistry, Faculty of Mathematics and Natural Sciences, Universitas Sumatera Utara, Jl. Bioteknologi No. 1, Medan 20155, Indonesia

Published online: 26 April 2023

acetophenone, and vanillin, that can efficiently enhance the thermodynamic stability of the bio-oil [8]. Two steps upgrading of bio-oil, i.e., esterification and HDO, has currently become a significant research area to develop alternative fuels and high-value chemicals [9]. In this case, catalyst is required to make the process faster and effective. So far, HDO process has been developed with numerous strategies, including base catalyzed [10].

Catalysts have played a hugely diverse range of theoretical and practical roles in the development of chemical industries and supporting economic growth since their first introduction to chemical reactions. Heterogeneous catalysts are the most used and developed type of catalysts. Metal-based heterogeneous catalyst, such as nickel (Ni), copper (Cu), rhodium (Rh), cobalt (Co), and iron (Fe) and more, has been developed for HDO process [11–14]. Cobalt (Co) is a promising catalyst [15], where cobalt oxide catalysts have demonstrated better catalytic performance in a number of reactions among many other transition metal oxides. However, the cobalt oxide catalysts still require modification to improve its catalytic activity, product selectivity, and stability of the catalysts. Iron metal (Fe) is a transition element that has a relatively empty d orbitals, which can increase the total number of active sites of the catalysts [16].

Catalysts can be manufactured by anchoring active metal components on the surface of carriers or support that have large surface areas. Condensation will result in an even distribution of metal across the entire surface of the catalyst and thus improving its overall properties. In comparison to catalysts with no carriers, catalysts with carriers have a better catalytic performance because of the increase in catalysts' surface areas and number of active sites due to the dispersion of active metals onto the catalysts' surface. Materials commonly used as support are silica [17], alumina [18, 19], zeolite [20, 21], and zirconia [22]. Due to its excellent deoxygenation capabilities, zeolite catalyst is the most frequently used catalyst in the biomass conversion process [23]. Mordenite is renowned for its exceptional properties, including high thermal stability, because of its ability to keep its structure at 800–900 °C. Mordenite is also ideal as an adsorbent, ion exchange medium, and carrier material because of the presence of voids and channels in its structure [24]. In this work, we aimed to produce heterogeneous catalyst using Co-Fe metal attached to mordenite catalyst by the impregnation method and upgrading bio-oil with two steps esterification and HDO-based transition metal oxides and mordenite catalyzed.

2 Experimental

2.1 Materials

The materials used in this study were synthetic mordenite type zeolite (HSZ-640HOA, Tosoh Corporation Japan, $SiO_2/Al_2O_3 = 9$), $FeCl_3{\cdot}6H_2O$ (E. Merck), $Co(NO_3)_2{\cdot}6H_2O$ (E. Merck), deionized water, ethanol p.a (E. Merck), H_2SO_4 (E. Merck), and KOH (E. Merck). Palm frond waste was obtained from PT. Perkebunan Nusantara II (Percut Sei Tuan district, North Sumatra, Indonesia).

2.2 Preparation of bio-oil

The conversion of palm frond waste into bio-oil was carried out by semi-fast pyrolysis method. The reactor used for semi-fast pyrolysis is a fixed-bed type reactor. The reactor schematic is shown in Fig. 1. First, the clean palm fronds are mashed into powder, 50 g of powder was put into a reactor. Next, the reactor was set at 500 °C at a heating rate of 1.3 °C/s. The process conditions used in the semi-fast pyrolysis method are carried out at 500 °C, a pressure of 0.1 MPa, and a residence time of 5 min. Then N_2 gas was flowed at an

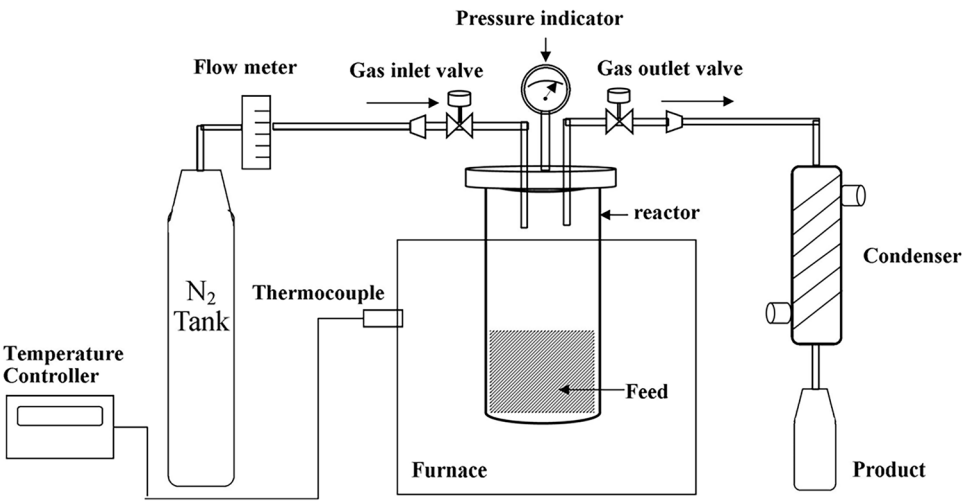

Fig. 1 Schematic of a fixed-bed reactor for a semi-fast pyrolysis process

adjusted flow rate of ±5 mL/s such that the powder would not be carried away by the gas flow.

2.3 Preparation of catalyst

Mordenite is thermally treated by calcining at 500 °C under an N_2 atmosphere. After that, metal impregnation was carried out by the reflux method. Catalyst was prepared by firstly dissolving Co precursor (0.5 g) in 500 mL deionized water in a round bottom flask followed by the addition of 100 g of mordenite into the mixture. The mixture was refluxed while constantly stirred at 600 RPM with a magnetic stirrer for 2 h at 80 °C. The condensate was oven-dried at 120 °C to obtain Co/Mor catalyst. Secondly, Co/Mor catalyst was combined into Fe metal precursor solution (1 g/L) and the mixture was refluxed while constantly stirred for 2 h at 80 °C. The condensate was dried in an oven at 120 °C, followed by oxidation process at 500 °C for 2 h with oxygen gas flow (±5 mL/s) to obtain Fe_2O_3-CoO/Mor catalyst.

2.4 Catalyst characterization

The crystallography of the catalyst was characterized using X-ray diffraction instrument (XRD Shimadzu 6100). Nitrogen adsorption-desorption test was carried out using gas sorption analyzer. Surface area was calculated using BET method, while pore volume and pore size were analyzed from the desorption band using BJH method. The component mapping of the produced catalyst was analyzed using scanning electron microscope with energy-dispersive X-ray spectroscopy model series (SEM-EDS Type Zeiss EPOMH 10Zss).

2.5 Upgrading process

The upgrading process of bio-oil is carried out in a fixed-bed reactor as reported by Sihombing et al. [25]. The reactor has a diameter of 5.5 cm with a height of 25 cm, a catalyst vessel with a diameter of 4.8 cm, and a height of 3.5 cm, while the furnace has a diameter of 40 cm and a height of 39 cm. The steam generated from the reaction is passed through a silicone hose and through the condenser to the product container. Bio-oil upgrading process is carried out in two stages, starting with esterification followed by the HDO process. Esterification procedure for bio-oil upgrading follows the method reported by Sondakh et al. [26], which started by mixing bio-oil and ethanol in a ratio of 1:1 (w/w) into the reactor at 60 °C for 2 h, followed by the HDO reaction with the presence of 1 g of catalyst for 50 g of bio-oils. Both catalyst and bio-oil were put into the fixed-bed reactor where N_2 gas was let to flow for 10 min to remove the oxygen content in the reactor. Next, the reactor was heated to 450 °C with H_2 gas flowing at 10 mL/min flow rate for 2 h. The product of the reaction was flowed to a cooling hose and weighed. The same procedure is repeated using a Fe_2O_3-CoO/Mor catalyst. The yield of the resulting product is calculated using the following formula.

$$Y\text{liquid } (\%) = \frac{Liquid\ fraction\ collected}{initial\ sample\ mass} \times 100\% \quad (1)$$

$$Y\text{coke } (\%) = \frac{coke\ \ fraction\ collected}{initial\ sample\ mass} \times 100\% \quad (2)$$

$$Y\text{gas } (\%) = 100\% - \left(Y_{\text{liquid}} + Y_{\text{coke}}\right) \quad (3)$$

2.6 Bio-oil characterization

The physicochemical properties of bio-oil before and after the esterification and HDO reactions were compared. The physical and chemical tests carried out were elemental analysis (C,H,N,O) using CHN Analyzer LECO-CHN 628, water content analysis using Metrohm 870 KF Titrano Plus, acid number determination using titration method, higher heating value (HHV) using Sheng and Azvedo formulas, component analysis using gas chromatography-mass spectrometry (GC-MS QP2010 Plus Shimadzu brand), and density and viscosity determination using gravimetric method and Ostwald viscometer.

3 Results and discussions

3.1 Catalyst crystallinity

The crystallinity of the catalyst samples was examined using the X-ray diffraction. The diffractograms obtained from mordenite and Fe_2O_3-CoO/Mor are compared in Fig. 2. The presence of high-intensity peaks is an indicative of crystalline materials [27]. In this study, synthetic mordenite catalyst used had 100% crystallinity, characterized by high diffraction peaks that were indicated by a narrow, sharp, and intense diffraction peaks located at 6.51; 9.68; 13.52; 19.70; 22.32; 25.69; and 27.62° (JCPDS 06-0239) [28].

The intensity of mordenite is affected by metal loading [29]. The crystallinity of the impregnated metal oxide catalyst is lower than that of pure mordenite. The main peaks of the two catalyst samples are formed in the same 2θ (degree) region with varying intensities. The formation of CoO crystal was indicated by the appearance of distinctive peak at 2θ = 30.5; 36.37; and 57.5° which is correlated with the data JCPDS files of 78-431, while the Fe_2O_3 crystal formed were characterized by the appearance of a distinctive peak at 2θ = 31.73; 52.46; and 47.45° in line with the data JCPDS

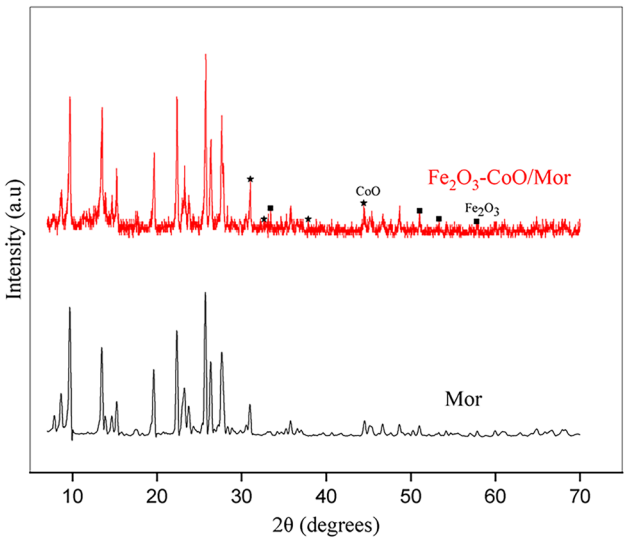

Fig. 2 Diffractogram of mordenite and Fe_2O_3-CoO/Mor catalysts

39-1346. The presence of metal oxides into mordenite catalyst did not damage its crystal structure, even though the peak intensity had changed.

3.2 Catalyst morphology and composition

Surface morphology of the catalysts as observed by SEM analysis is shown in Fig. 3. The SEM micrograph of mordenite showed the presence of different particles which sized varies with the voids between particles. Meanwhile, the surface morphology of Fe_2O_3-CoO/Mor is denser than mordenite.

The results demonstrated that the metals have been evenly distributed throughout the surfaces of mordenite. The average particle diameters of mordenite and Fe_2O_3-CoO/Mor catalysts were 361 nm and 723 nm, respectively. The composition of each catalyst was analyzed using EDX (Table 1). The decrease in Si and Al content of Fe_2O_3-CoO/Mor indicates changes that occur during the metal impregnation, calcination, and oxidation processes. Calcination involved high temperatures process that could cause some of the Si and Al constituents of the skeleton to be separated from the mordenite framework. The increase in the percentage of O is due to the oxidation process that forms the transition metal into its oxide form [30].

Table 1 Mordenite and Fe_2O_3-CoO/Mor catalysts composition

Components	Mordenite (mass%)	Fe_2O_3-CoO/Mor (mass%)
Si	36.67	30.81
Al	3.15	2.99
O	55.01	57.84
C	4.02	7.78
Fe	-	0.38
Co	-	0.20
Impurities	1.14	-
Si/Al	11.64	10.30

The Fe and Co metals added to the mordenite to form Fe_2O_3-CoO/Mor catalyst were quantified at 0.38 and 0.2 wt%, respectively. The distribution of Fe and Co metals on the catalyst surface was observed using the SEM-EDX elemental mapping analysis shown in Fig. 4. The two metals are not clearly observed due to its small amount. The elemental distribution shows that the morphology is dominated by Si, Al, and O. The mapping results were in line with EDX data. Impurities in the form of Ni and Cu elements were found in mordenite, but not in Fe_2O_3-CoO/Mor catalyst. Processes, including impregnation, calcination, and oxidation, in the preparation of Fe_2O_3-CoO/Mor catalyst have removed the impurities.

3.3 Nitrogen gas sorption analysis

The graph of the adsorption-desorption isotherm of each catalyst is shown in Fig. 5. Following the IUPAC classification, the isotherm of Mor and Fe_2O_3-CoO/Mor is classified into type IV with a hysteresis loop at P/P_0 between 0.4 and 0.9. The presence of a hysteresis loop on the isotherm graph indicates that the material contains mesoporous (2–50 nm) [31].

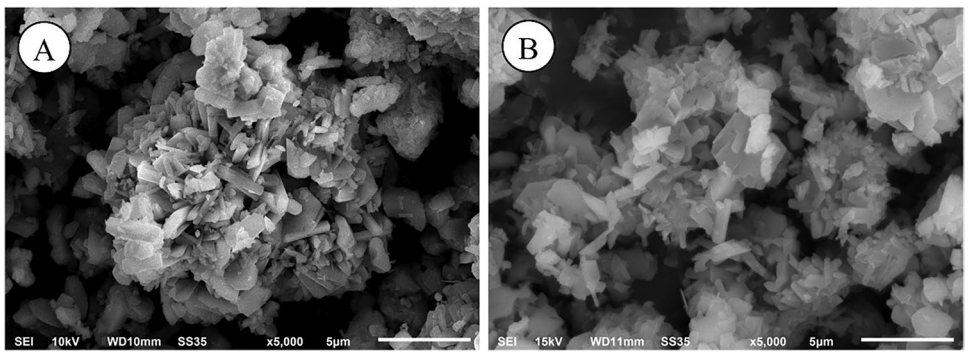

Fig. 3 Surface morphology of **A** Mor and **B** Fe_2O_3-CoO/Mor catalysts

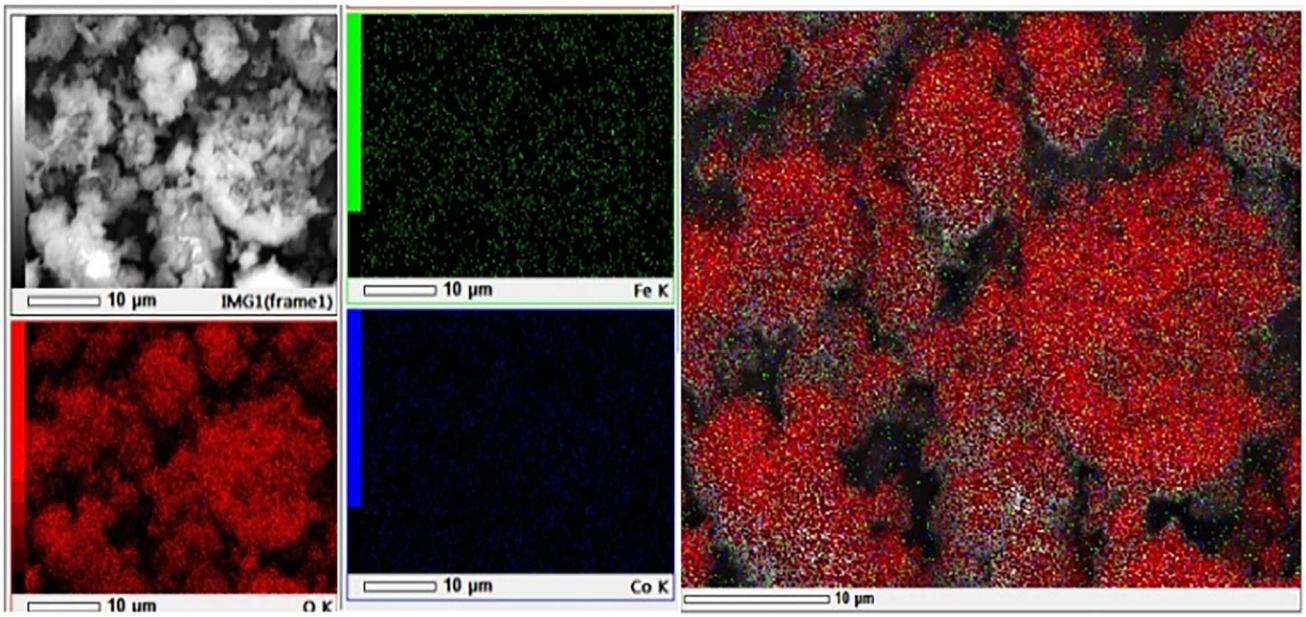

Fig. 4 Elemental mapping of Fe_2O_3-CoO/Mor catalyst. The distribution of elements shows different colors for oxygen with red color, iron with green color, and cobalt with blue color

The surface area measurement, total volume, and pore diameters of the catalyst samples are summarized in Table 2. The surface area was calculated using BET method, while the total pore volume and pore diameter were analyzed by the desorption band using BJH method.

Fe_2O_3-CoO/Mor catalysts had slightly lower surface area and total pore volume, but slightly larger pore diameter when compared with mordenite. Thermal processing and loading of metal oxides on mordenite has changed the surface and pores of the mordenite catalyst. The calcination process removes organic impurities in the pores, hence the improvement in the pore sizes and catalyst characteristic [32]. The presence of metal oxides can increase the number of active sites of mordenite which can improve the catalytic performance of the catalyst.

3.4 Constituent of the raw bio-oil

Pyrolysis at a high temperature causes various compounds to decompose into other compounds. The conversion of biomass in the pyrolysis process goes through various mechanisms, such as char formation, depolymerization, or fragmentation. The formation of char consists of the conversion of biomass in solid residues which present an aromatic polycyclic structure. Depolymerization consists of bond breaking between polymer monomer units. Fragmentation consists of breaking the covalent bonds of the polymer, even within monomer units, and results in the formation of non-condensable gases [33]. Therefore, an analysis was carried out to determine the compounds formed after the pyrolysis process.

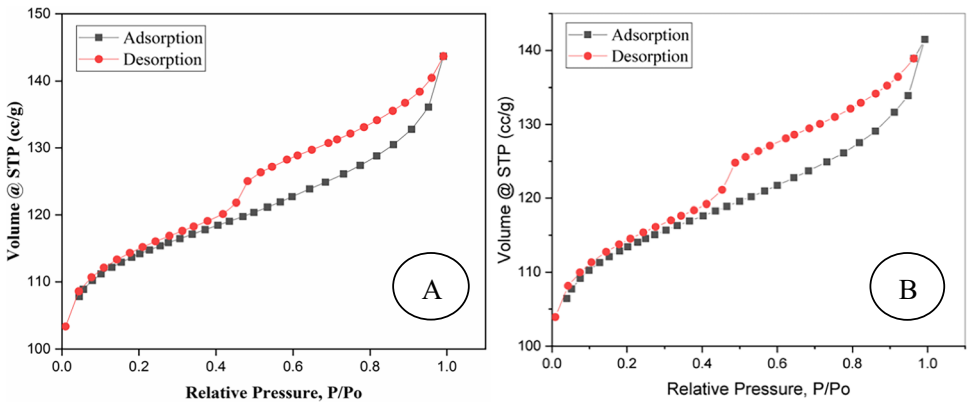

Fig. 5 N_2 adsorption-desorption isotherm graphs of **A** Mor and **B** Fe_2O_3-CoO/Mor catalysts

Table 2 Surface area and pore volume and diameters of mordenite and Fe_2O_3-CoO/Mor catalysts

Catalyst	Surface area (m^2/g)	Pore volume (cc/g)	Pore diameter (nm)
Mor	415.8	0.056	3.755
Fe_2O_3-CoO/Mor	415.3	0.053	3.782

The bio-oil obtained from the pyrolysis of palm frond was analyzed for its compound content using GC-MS analysis. The detected compounds were grouped into several groups of compounds such as acids, ketones, furans, aldehydes, and phenols which are summarized in Table 3.

Based on Table 3, the bio-oil content is dominated by furans, ketones, aldehydes, and acids. These compounds are the result of the decomposition of lignocellulose, where cellulose produces furan and ketone groups, hemicelluloses produce many acids and ketones, while lignin produces phenols [34]. These results prove that cellulose and hemicellulose are the most abundant components in palm frond. This is in agreement with previous study which reported that the composition of lignocellulose in biomass generally ranged from 40 to 50 wt% for cellulose, 20 to 40 wt% for hemicellulose, and 10 to 40 wt% for lignin [35].

3.5 Bio-oil upgrading

The HDO process was carried out on raw bio-oil and esterified bio-oil. Esterification can reduce the acidity of bio-oil by adding polar solvents such as ethanol. It can also reduce the density and viscosity and increase the calorific value of bio-oil [36]. The HDO process is carried out to reduce oxygenated compounds in bio-oil to obtain a more stable compound [37]. In this study, a comparison was made between the direct HDO method and the two-step method that combines the esterification and HDO steps. Upgrading of bio-oil with these two methods was carried out using Mor and Fe_2O_3-CoO/Mor catalysts. The resulting yield distribution is shown in Fig. 6.

Table 3 Composition of bio-oil compounds from palm frond

Group	Compound	Area (%)
Furans	2-Furancarboxaldehyde	38.59
	2-Furancarboxaldehyde, 5-methyl-	2.28
		40.87
Phenols	Phenol	4.76
	Phenol, 2-methoxy-	0.39
	Phenol, 2,6-dimethoxy-	1.27
		6.42
Ketones	2-Cyclopenten-1-one, 2-hydroxy-3-methyl	0.74
	Cyclopentadecanone, 2-hydroxy-	15.65
		16.39
Acids	Pentadecanoic acid	1.98
	Hexadecanoic acid	12.42
	9-Octadecenoic acid	2.71
		17.11
Aldehydes	Tridecanedial	0.43
	9-Octadecenal	15.88
		16.31

Based on Fig. 6, in general, more liquid phase is produced from the two-stage esterification-HDO method than using the direct HDO method. The Brønsted acid site contained in mordenite has an important role during the HDO process, especially for reducing the oxygen content through the deoxygenation pathway, the presence of the Brønsted acid site can provide protons (H^+) to break the O atom bond in the OH group through a dehydration reaction and produce H_2O. Less residue is left when using the two-step method, which indicates a more complete reaction. The esterification step showed a positive impact as a pre-treatment for the bio-oil sample. The conversion was found to be even better when using Fe_2O_3-CoO/Mor as a catalyst. The presence of metal oxide active sites increases the activity of the catalyst to catalyze the bio-oil during the HDO reaction. Grioui et al. [38] explained that the presence of Fe_2O_3 causes the gas produced from the reaction to be inhibited by the condensation reaction and thus moving the gas between the catalyst particles that would result in the increasing residence time for the conversion of the condensed gas and liquid phase products. In addition, there was a decrease in coke formation indicating that the Fe_2O_3-CoO catalyst was effective in inhibiting polymerization and polycondensation reactions [12]. The resulting liquid phase was then analyzed

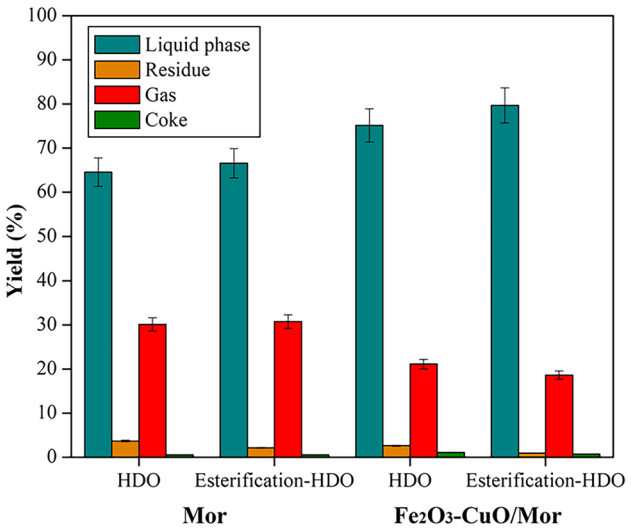

Fig. 6 Product distribution of HDO of bio-oil using Mor and Fe_2O_3-CoO/Mor catalysts

Table 4 Physicochemical properties of raw bio-oil, HDO bio-oil, and esterification-HDO bio-oil

Properties	Raw bio-oil	HDO	Esterification-HDO
Elemental analysis (wt%)			
C	11.5	17.8	23.5
H	9.76	10.3	11.2
N	0.04	0.03	0.03
O[a]	78.7	71.9	65.2
Water content (%)	75.2	50.1	45.2
Density (g/cm^3)	1.03	1.01	0.93
HHV (MJ/kg)[b]	11.6	13.7	16.0
Viscosity (cP)	1.13	1.10	1.14
Acid number (mg KOH/g oil)	124	112	64
H/C	10.2	6.94	5.69
O/C	5.15	3.04	2.07
DOD (%)	-	40.9	59.8

[a]Calculated by difference in percentage

[b]High heating value was calculated by using the following formula: HHV (MJ/ kg) = −1.3675 + (0.3137 C) + (0.7009 H) + (0.0318 O)

further to determine its physicochemical properties. These properties are compared with the properties of raw bio-oil resulting from pyrolysis and are summarized in Table 4.

Based on Table 4, there is a change in the physicochemical properties of bio-oil after undergoing the upgrading process, either through the direct HDO method or the two-stage esterification-HDO method. Elemental analysis showed that the upgrading process succeeded in increasing the percentages of C and H, as well as reducing O levels. The magnitude of the decrease in O levels can be shown by calculating the degree of deoxygenation (DOD), where the DOD values for the HDO and esterification-HDO methods are determined to be 40.9% and 59.8%, respectively. In addition, the molar ratio of H/C and O/C can also be determined which could be used to estimate the tendency of the dominant reaction pathway to be traversed during the upgrading process. In this case, for both methods, there was a decrease in the O/C and H/C molar ratios. This indicates the deoxygenation or demethoxylation pathway is preferable over the hydrogenation pathway. Through this reaction pathway, a decrease in O levels can occur due to the release of O as a by-product in the form of H_2O or CO_2. This assumption is supported by GC-MS data which shows the compounds contained in bio-oil. With this analysis, elemental data can also be calculated HHV. HHV bio-oil after upgrading process increased from 11.6 to 13.7 MJ/kg (HDO method), and 16.0 MJ/kg (esterification-HDO method). The 38% increase in HHV value was recorded for the upgraded bio-oils.

Other physicochemical properties that change during the upgrading process are moisture content, density, viscosity, and acid number. The density of bio-oil decreased slightly due to the reduction of large-molecular organic compounds that were converted during the reaction. However, the viscosity of the bio-oil hardly changed. Meanwhile, the water content was reduced by up to a third due to the release of water molecules during the reaction at high temperatures. This also supports the reason for the increase in HHV bio-oil after treatment. Moreover, the acid number is drastically reduced by half, especially in the HDO-esterification method. This value shows the positive role of the esterification process as the initial stage of the bio-oil upgrading processes. Decreased acid content provides better stability for bio-oil.

3.6 Constituent of upgraded bio-oil

The compounds contained in the bio-oil after the upgrading process were analyzed using GC-MS. The compounds contained in bio-oil were categorized into several groups, such as acids, aldehydes, furans, esters, ketones, and phenols, as shown in Fig. 7.

Based on the results from the GC-MS analysis, the compounds in raw bio-oil were dominated by cellulose derivatives including aldehydes, furan, ketones, and lignin derivatives [39]. The upgrading process starting with the esterification stage produces several different components. The esterification step plays an important role in converting acids into esters [40, 41], which is supported by the high percentage of esters up to 30%. By reducing the acids contained in the bio-oil, the stability of the bio-oil improves. This HDO-esterification method also has an impact on the transformation pathway of furfural compounds (Fig. 8). In this study, furan was one of the dominant compounds found. In the HDO-esterification stage, furfural can go through several reaction pathways as shown in Fig. 8. Furfural undergoes cracking causing the furfural bond

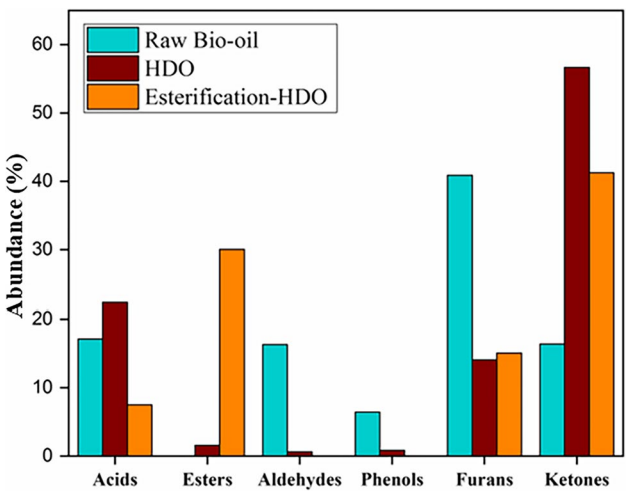

Fig. 7 Bio-oil compound composition after esterification and HDO

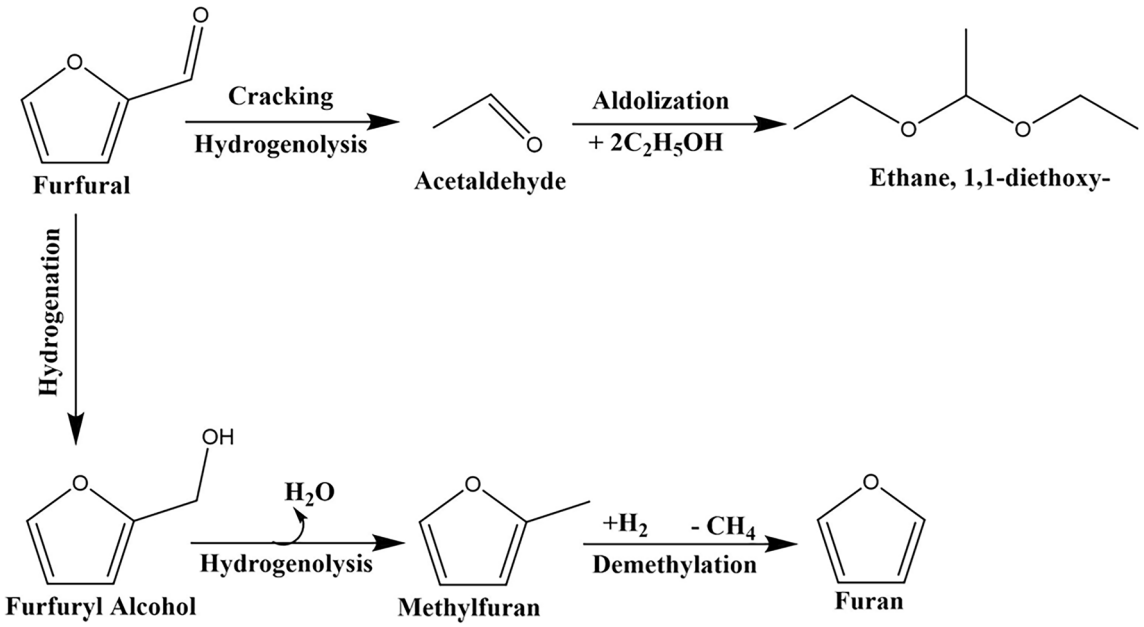

Fig. 8 Possible reactions pathways in furfural esterification-HDO process

to break to form acetaldehyde, then in the presence of ethanol, acetaldehyde can undergo aldolization to form ethane,1,1-diethoxy [42]. This compound is an acetal group that can be applied as an organic solvent, starting material for organic synthesis, and fuel additive [43–45]. Furfural can also undergo hydrogenation to produce furfuryl alcohol, then through the hydrogenolysis pathway, it produces methylfuran which can then undergo demethylation to release CH_4 to produce furan compounds [46]. Methylfuran is an important chemical compound that has the potential to be used as a fuel component, and as an intermediate in various pharmaceutical and perfume industries [47, 48]. In addition, the ketone group is the most dominant product content. Ketones can be obtained from the rearrangement of furfuryl alcohol in the presence of hydrogen [49] or could also be obtained from ring opening of methylfuran to form open chain ketones [50]. This is supported by the reduced furans content during the upgrading process. In addition, phenol content which was not found after the esterification-HDO bio-oil process could occur because phenol had been converted to cyclohexanone as a ketone group. The mechanism for the formation of cyclohexanone is shown in Fig. 9.

As for the bio-oil which only undergoes one stage of the process through direct HDO, only a very small amount of hydrocarbon compounds are formed in the form of octadecene (0.16%). The presence of octadecene may result from the dehydration of octadecanoic acid contained in the raw bio-oil, through the deoxygenation pathway to produce octadecanal, then through the hydrogenation pathway and undergo hydrogenolysis to produce octadecene [51]. This cannot be separated from the role of the catalyst, where the presence of Fe oxide can catalyze the hydrogenation of the C=O bond and inhibit the breaking of the C-C bond during the HDO process. Iron-bearing in the catalyst played important roles by increasing the interaction between Co oxide and mordenite, which stabilized Fe_2O_3-CoO/Mor catalyst during bio-oil HDO reaction. The better the interaction between Co oxide and mordenite, the better the adsorption of oxygenated compounds from raw bio-oil by Fe_2O_3-CoO/Mor catalyst. As a result, there was a notable increase in the conversion reaction rate of the absorbed oxygenated compounds to the desired hydrocarbon compounds [12].

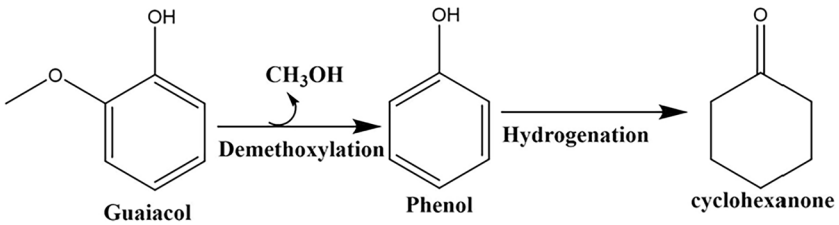

Fig. 9 Possible reaction pathways in HDO of guaiacol

4 Conclusions

Upgrading bio-oil using Fe_2O_3-CoO/Mor catalyst with two stages of esterification-HDO has improved the physicochemical properties of bio-oil compared to the one-stage upgrading process. Product analysis showed that the content of C and H increased from 11.5 to 23.5 wt%, and from 9.76 to 11.2 wt%, while O decreased from 78.7 to 65.2 wt% with a degree of deoxygenation of 59.8%. Moreover, HHV increased by 38% from 11.6 to 16.0 MJ/kg. Mixed metal oxide loaded on mordenite increases the number of active sites of the catalyst thereby increasing the catalytic performance in the HDO process with the catalyst. Meanwhile, esterification provides an active role in reducing acidity by converting carboxylic acids into their ester forms. The upgrading process goes through various reaction pathways, such as hydrogenation, deoxygenation, demethylation, aldolization, and rearrangement. The octadecene hydrocarbon product is produced through the HDO process. In addition, various high-value chemicals are obtained during the upgrading process, such as methylfuran and ethane,1,1-diethoxy.

Author contribution ANP: conceptualization, methodology, data curation, investigation, writing — original draft. RG: conceptualization, formal analysis, writing — original draft. AK: formal analysis, data curation, writing — review and editing. NN: formal analysis, writing — review and editing. JLS: formal analysis, data curation, writing — original draft. SG: supervision, data curation, writing — review and editing. HRW: visualization, investigation, writing — review and editing. MIH: visualization, investigation, writing — review and editing. RR: software, writing — review and editing. AIYT: supervision, formal analysis, data curation, writing — review and editing.

Funding The authors would like to acknowledge the Institute for Research and Community Service (LPPM) Universitas Negeri Medan for the financial support provided through the 2022 Applied Product Research Scheme with grant number no. 104/UN33.8/KEP/PPKM/PT/2022.

Data availability The datasets generated during and/or analyzed during the current study are available from the corresponding author on reasonable request.

Declarations

Ethical approval Not applicable.

Competing interests The authors declare no competing interests.

References

1. Kim SW, Koo BS, Ryu JW et al (2013) Bio-oil from the pyrolysis of palm and Jatropha wastes in a fluidized bed. Fuel Process Technol 108:118–124. https://doi.org/10.1016/j.fuproc.2012.05.002
2. Zong R, Li H, Ding WT, Huang H (2021) Highly dispersed Pd on zeolite/carbon nanocomposites for selective hydrodeoxygenation of biomass-derived molecules under mild conditions. ACS Sustain Chem Eng 9:9891–9902. https://doi.org/10.1021/acssuschemeng.1c02876
3. Bridgwater AV (2012) Review of fast pyrolysis of biomass and product upgrading. Biomass Bioenergy 38:68–94. https://doi.org/10.1016/j.biombioe.2011.01.048
4. Hu X, Gunawan R, Mourant D et al (2017) Upgrading of bio-oil via acid-catalyzed reactions in alcohols — a mini review. Fuel Process Technol 155:2–19. https://doi.org/10.1016/j.fuproc.2016.08.020
5. Wang L, Zhang M, Zhang M et al (2013) Hydrodeoxygenation of dibenzofuran over mesoporous silica COK-12 supported palladium catalysts. Energy Fuel 27:2209–2217. https://doi.org/10.1021/ef302166q
6. Oasmaa A, Kuoppala E (2003) Fast pyrolysis of forestry residue. 3. Storage stability of liquid fuel. Energy Fuel 17:1075–1084. https://doi.org/10.1021/ef030011o
7. Ciddor L, Bennett JA, Hunns JA et al (2015) Catalytic upgrading of bio-oils by esterification. J Chem Technol Biotechnol 90:780–795. https://doi.org/10.1002/jctb.4662
8. Jiang J, Ding W, Li H (2021) Promotional effect of F for Pd/HZSM-5 catalyst on selective HDO of biobased ketones. Renew Energy 179:1262–1270. https://doi.org/10.1016/j.renene.2021.07.065
9. Huang H, Zong R, Li H (2020) Synergy effects between oxygen groups and defects in hydrodeoxygenation of biomass over a carbon nanosphere supported Pd catalyst. ACS Sustain Chem Eng 8:15998–16009. https://doi.org/10.1021/acssuschemeng.0c06122
10. Li L, Dong L, Li D et al (2020) Hydrogen-free production of 4-alkylphenols from lignin via self-reforming-driven depolymerization and hydrogenolysis. ACS Catal 10:15197–15206. https://doi.org/10.1021/acscatal.0c03170
11. Zhang L, Shang N, Gao S et al (2020) Atomically dispersed Co catalyst for efficient hydrodeoxygenation of lignin-derived species and hydrogenation of nitroaromatics. ACS Catal 10:8672–8682. https://doi.org/10.1021/acscatal.0c00239
12. Cheng S, Wei L, Julson J, Rabnawaz M (2017) Upgrading pyrolysis bio-oil through hydrodeoxygenation (HDO) using non-sulfided Fe-Co/SiO2 catalyst. Energ Conver Manage 150:331–342. https://doi.org/10.1016/j.enconman.2017.08.024
13. Hočevar B, Grilc M, Likozar B (2019) Aqueous dehydration, hydrogenation, and hydrodeoxygenation reactions of bio-based mucic acid over Ni, NiMo, Pt, Rh, and Ru on neutral or acidic catalyst supports. Catalysts 9:286. https://doi.org/10.3390/catal9030286
14. Bjelić A, Grilc M, Likozar B (2020) Bifunctional metallic-acidic mechanisms of hydrodeoxygenation of eugenol as lignin model compound over supported Cu, Ni, Pd, Pt, Rh and Ru catalyst materials. Chem Eng J 394:124914. https://doi.org/10.1016/j.cej.2020.124914
15. Mei J, Zhao S, Xu H et al (2016) The performance and mechanism for the catalytic oxidation of dibromomethane (CH2Br2) over Co3O4/TiO2 catalysts. RSC Adv 6:31181–31190. https://doi.org/10.1039/c6ra00372a
16. Satterfield C (1980) Heterogenous catalyst in practice. Mc Graw Hill Book, New York
17. Delucia NA, Jystad A, Vander LK et al (2019) Silica supported molecular palladium catalyst for selective hydrodeoxygenation of aromatic compounds under mild conditions. ACS Catal 9:9060–9071. https://doi.org/10.1021/acscatal.9b02460
18. Vikár A, Solt HE, Novodárszki G et al (2021) A study of the mechanism of triglyceride hydrodeoxygenation over alumina-supported and phosphatized-alumina-supported Pd catalysts. J Catal 404:67–79. https://doi.org/10.1016/j.jcat.2021.08.052
19. Phan DP, Vo TK, Le VN et al (2020) Spray pyrolysis synthesis of bimetallic NiMo/Al2O3–TiO2 catalyst for hydrodeoxygenation of guaiacol: effects of bimetallic composition and reduction temperature. J Ind Eng Chem 83:351–358. https://doi.org/10.1016/j.jiec.2019.12.008
20. Lee CW, Lin PY, Chen BH et al (2021) Hydrodeoxygenation of palmitic acid over zeolite-supported nickel catalysts. Catal Today 379:124–131. https://doi.org/10.1016/j.cattod.2020.05.013

21. Luo W, Cao W, Bruijnincx PCA et al (2019) Zeolite-supported metal catalysts for selective hydrodeoxygenation of biomass-derived platform molecules. Green Chem 21:3744–3768. https://doi.org/10.1039/c9gc01216h
22. He Y, Bie Y, Lehtonen J et al (2019) Hydrodeoxygenation of guaiacol as a model compound of lignin-derived pyrolysis bio-oil over zirconia-supported Rh catalyst: process optimization and reaction kinetics. Fuel 239:1015–1027. https://doi.org/10.1016/j.fuel.2018.11.103
23. Usui K, Kidena K, Murata S, Nomura M, Trisunaryanti W (2004) Catalytic hydrocracking ofpetroleum-derived asphaltenes by transition metal-loaded zeolite catalysts. J Fuel 83:1899–1906
24. Trisunaryanti W, Triyono, Wijaya K, Majid AB, Priastomo Y, Febriyanti E, Syafitri, Hasyyati, Nugroho A (2012) Characterization and activity test of mordenite and Y-zeolite catalysts in hydrocracking of tire waste to fuel fractions. Prosiding Seminar Nasional Kimia Unesa
25. Sihombing JL, Herlinawati H, Pulungan AN et al (2023) Effective hydrodeoxygenation bio-oil via natural zeolite supported transition metal oxide catalyst. Arab J Chem 16(6):104707. https://doi.org/10.1016/j.arabjc.2023.104707
26. Sondakh RC, Hambali E, Indrasti NS (2019) Improving characteristic of bio-oil by esterification method. IOP Conf Ser Earth Environ Sci 230:012071. https://doi.org/10.1088/1755-1315/230/1/012071
27. Pulungan AN, Nurfajriani KA et al (2022) The stabilization of bio-oil as an alternative energy source through hydrodeoxygenation using Co and Co-Mo supported on active natural zeolite. J Phys Conf Ser 2193:012084. https://doi.org/10.1088/1742-6596/2193/1/012084
28. Vasconcelos SC, Pinhel LFC, Madriaga VGC et al (2022) Selective synthesis of levulinic ester from furfural catalyzed by hierarchical zeolites. Catalysts 12:1–18. https://doi.org/10.3390/catal12070783
29. Gea S, Irvan WK et al (2022) Bio-oil hydrodeoxygenation over zeolite-based catalyst: the effect of zeolite activation and nickel loading on product characteristics. Int J Energy Environ Eng 13:541–553. https://doi.org/10.1007/s40095-021-00467-0
30. Pulungan AN, Kembaren A, Nurfajriani N et al (2021) Biodiesel production from rubber seed oil using natural zeolite supported metal oxide catalysts. Polish J Environ Stud 30:5681–5689. https://doi.org/10.15244/pjoes/135615
31. Sihombing JL, Gea S, Wirjosentono B et al (2020) Characteristic and catalytic performance of Co and Co-Mo metal impregnated in sarulla natural zeolite catalyst for hydrocracking of MEFA rubber seed oil into biogasoline fraction. Catalysts 10:121
32. Djaeni M, Kurniasari L, Sasongko SB (2015) Preparation of natural zeolite for air dehumidification in food drying. Int J Sci Eng (IJSE) 8:80–83. https://doi.org/10.12777/ijse.8.2.80-83
33. Collard FX, Blin J (2014) A review on pyrolysis of biomass constituents: mechanisms and composition of the products obtained from the conversion of cellulose, hemicelluloses and lignin. Renew Sustain Energy Rev 38:594–608. https://doi.org/10.1016/j.rser.2014.06.013
34. Zhao C, Jiang E, Chen A (2017) Volatile production from pyrolysis of cellulose, hemicellulose and lignin. J Energy Inst 90:902–913. https://doi.org/10.1016/j.joei.2016.08.004
35. Zadeh ZE, Abdulkhani A, Aboelazayem O, Saha B (2020) Recent insights into lignocellulosic biomass pyrolysis: a critical review on pretreatment, characterization, and products upgrading. Processes 8:799. https://doi.org/10.3390/pr8070799
36. Xu Y, Zhang L, Lv W et al (2021) Two-step esterification–hydrogenation of bio-oil to alcohols and esters over raney ni catalysts. Catalysts 11:1–10. https://doi.org/10.3390/catal11070818
37. Gea S, Hutapea YA, Piliang AFR et al (2022) A comprehensive review of experimental parameters in bio-oil upgrading from pyrolysis of biomass to biofuel through catalytic hydrodeoxygenation. BioEnergy Res 1–23. https://doi.org/10.1007/s12155-022-10438-w
38. Huang Z, Qin L, Xu Z et al (2019) The effects of Fe2O3 catalyst on the conversion of organic matter and bio-fuel production during pyrolysis of sewage sludge. J Energy Inst 92:835–842. https://doi.org/10.1016/j.joei.2018.06.015
39. Grioui N, Halouani K, Agblevor FA (2014) Bio-oil from pyrolysis of Tunisian almond shell: comparative study and investigation of aging effect during long storage. Energy Sustain Dev 21:100–112. https://doi.org/10.1016/j.esd.2014.05.006
40. Lee HW, Jeong H, Ju YM, Lee SM (2020) Upgrading of bio-oil by ex-situ catalytic pyrolysis and in-line esterification in fluidized bed reactor. Korean J Chem Eng 37:1174–1180. https://doi.org/10.1007/s11814-020-0527-0
41. Suota MJ, Simionatto EL, Scharf DR et al (2019) Esterification, distillation, and chemical characterization of bio-oil and its fractions. Energy Fuel 33:9886–9894. https://doi.org/10.1021/acs.energyfuels.9b01971
42. Wang J, Luo Z, Zhang J et al (2011) Reactions of furfural and acetic acid as model compounds for bio-oil upgrading in supercritical ethanol. In: 2011 International Conference on Electronics, Communications and Control (ICECC), vol 2. IEEE, Ningbo, China, pp 1587–1592. https://doi.org/10.1109/ICECC.2011.6067982
43. Zhang H, Wu Y, Li L, Zhu Z (2015) Photocatalytic direct conversion of ethanol to 1,1-diethoxyethane over noble-metal-loaded TiO2 nanotubes and nanorods. ChemSusChem 8:1226–1231. https://doi.org/10.1002/cssc.201403305
44. Kawaguchi D, Ogihara H, Kurokawa H (2021) Upgrading of ethanol to 1,1-diethoxyethane by proton-exchange membrane electrolysis. ChemSusChem 14:4431–4438. https://doi.org/10.1002/cssc.202101188
45. He X, Liu H (2014) Efficient synthesis of 1,1-diethoxyethane via sequential ethanol reactions on silica-supported copper and H-Y zeolite catalysts. Catal Today 233:133–139. https://doi.org/10.1016/j.cattod.2014.01.023
46. Gilkey MJ, Panagiotopoulou P, Mironenko AV et al (2015) Mechanistic insights into metal lewis acid-mediated catalytic transfer hydrogenation of furfural to 2-methylfuran. ACS Catal 5:3988–3994. https://doi.org/10.1021/acscatal.5b00586
47. Toledo F, Ghampson IT, Sepúlveda C et al (2019) Effect of Re content and support in the liquid phase conversion of furfural to furfuryl alcohol and 2-methyl furan over ReOx catalysts. Fuel 242:532–544. https://doi.org/10.1016/j.fuel.2019.01.090
48. Jaatinen SK, Karinen RS, Lehtonen JS (2017) Liquid phase furfural hydrotreatment to 2-methylfuran with carbon supported copper, nickel, and iron catalysts. ChemistrySelect 2:51–60. https://doi.org/10.1002/slct.201601947
49. Moravvej Z, Farshchi Tabrizi F, Rahimpour MR (2021) Vapor phase conversion of furfural to valuable biofuel and chemicals over alumina-supported catalysts: screening catalysts. Top Catal:1–14. https://doi.org/10.1007/s11244-021-01470-9
50. Byun MY, Park DW, Lee MS (2020) Effect of oxide supports on the activity of PD based catalysts for furfural hydrogenation. Catalysts 10:837. https://doi.org/10.3390/catal10080837
51. Li J, Zhang J, Wang S et al (2019) Chemoselective hydrodeoxygenation of carboxylic acids to hydrocarbons over nitrogen-doped carbon-alumina hybrid supported iron catalysts. ACS Catal 9:1564–1577. https://doi.org/10.1021/acscatal.8b04967